Electronic Supplementary Material (ESI) for Journal of Materials Chemistry A.

Supporting Information

An Adaptive and Stable Bio-Electrolyte for Rechargeable Zn-Ion Batteries

Silan Zhang,[a,b] *Nengsheng Yu,*[b] *Sha Zeng,*[b] *Susheng Zhou,*[b] *Minghai Chen,*[b] *Jiangtao Di**[b] *and Qingwen Li**[a,b]

[a] School of Physical Science and Technology, ShanghaiTech University, Shanghai 201210, China
[b] Key Laboratory of Nanodevices and Applications, Suzhou Institute of Nano-Tech and Nano-Bionics, Chinese Academy of Sciences, Suzhou 215123, China

Experimental Section

Synthesis of Electrode Materials

a. Materials

Flexible multi-walled CNT film was prepared by FCCVD method and was provided by Suzhou Creative Nano Carbon Co., Ltd. All of other agents were analytical reagent and purchased from Aladdin Industrial Co., Ltd. (China).

b. Synthesis of MnO_2/CNT hybrid film

As-received pristine CNT films prepared by floating catalytic chemical vapor deposition were pretreated by immersing in 12 M HCl and keep at 60 °C for 4 h to make the CNT surface hydrophilic. Manganese dioxide was electrodeposited by a cyclic voltammetry technique in the electrolyte composed of 0.1 M Na_2SO_4 and 0.1 M $Mn(CH_3COO)_2$, using a hydrophilized CNT film as working electrode, a saturated calomel electrode (SCE) as reference electrode, and a Pt sheet as counter electrode, respectively. The potential range was between +0.3 V and +0.6 V versus SCE at a scanning speed of 250 mV s^{-1} for 2,000 cycles. The prepared MnO_2/CNT composite films were then calcined at 200 °C for 10 hours. The deposited MnO_2 has a mass loading of 0.5 mg/cm^2, which was measured using a micro balance (Mettler Toledo, model: XP2U). The mass ratio of MnO_2 and CNT film is 1:1.

Preparation of gum electrolytes

Xanthan gum electrolytes were prepared by dissolving as-received xanthan gum powder in the aqueous solutions of $ZnSO_4$ and $MnSO_4$. The xanthan gum powder used in the present study were purchased from Aladdin (UPS class). For the gum electrolyte used for the battery assembling, we dissolved 10 g of xanthan gum powder in 50 mL aqueous solution of 2 M $ZnSO_4$ and 0.1 M $MnSO_4$ solution at room temperature followed by magnetic stirring after 30 min. The PH of the as prepared gum electrolyte is about 4.

Assembling of Zn–MnO_2 batteries

A zinc foil (purity: 99.99%) that was cut into 2-cm-wide and 30-µm-thick, was used as the anode. A 15-µm-thick MnO_2/CNT composite film was used as the cathode. A very thin layer of the xanthan gum electrolyte was then coated on the electrodes, followed by attaching the cathode electrode on the anode. Due to the high viscosity of the employed gum electrolyte, separator was not used in our batteries. Both anode and cathode were wired by a nickel strip for battery testing. After that, the battery was sealed by hot-pressing two pieces of polyethylene oxide films. The active area of the tested batteries was about 2×2 cm^2. The areal densities are 1 mg/cm^2, 0.75 mg/cm^2, 1.738 mg/cm^2 for the cathode, anode, and gum electrolyte, respectively.

Materials characterization

Morphology characterization of the investigated samples was performed using SEM (Quanta 400 FEG, FEI) and HRTEM (Tecnai G2 F20 S-Twin, FEI). The XRD data were collected by D8 Advance Powder X-ray diffractometer (Bruker AXS) and Raman spectra were collected by a LabRAM HR Raman spectrometer. The GPC data were collected by Agilent PL-GPC 50 System.

Electrochemical test

Cyclic voltammetry and electrochemical impedance spectroscopy were conducted on a CHI 660C potentiostat. For impedance measurements on gum electrolytes, a piece of gum was placed between two stainless steels having an area of 4.1 cm^2, and then the gum was uniformly compressed into a 0.21-cm-thick film. Impedance measurements were carried out between 10 kHz to 0.01 Hz with an AC amplitude of 10 mV. The real impedances at the highest frequency were taken as the bulk resistance. The galvanostatic charge/discharge measurements was carried out on a LANHER battery tester (Wuhan). The specific capacity, energy density, and power density were calculated based on the mass of MnO_2. The energy density (E) of the battery was calculated by: $E=\int_0^t IV_t dt/m$, and the power density was calculated by $P=E/t$, where I is discharge current, $V(t)$ is the discharge voltage at t, and m is the mass of the cathode.

Supplementary Figures

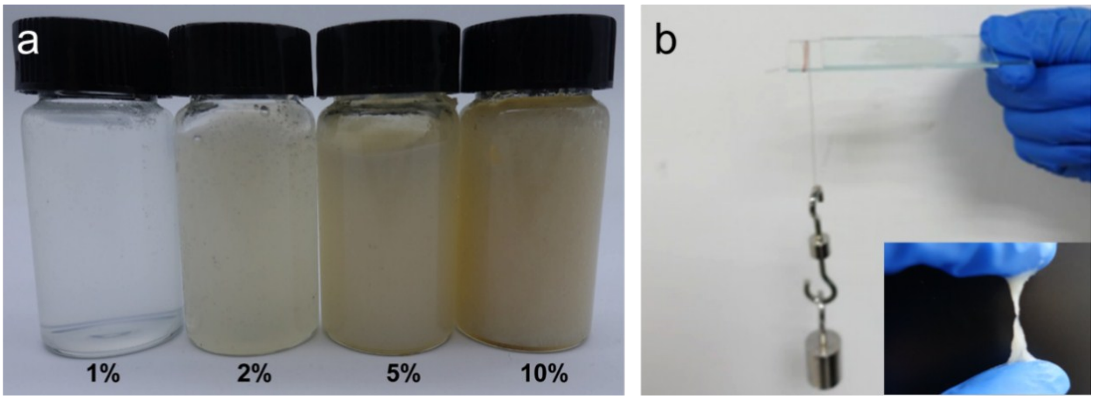

Figure S1. a) Digital photographs of 2 M $ZnSO_4$/0.1 M $MnSO_4$ electrolytes with different weight percentages of xanthan gum. b) The gum electrolyte (2 M $ZnSO_4$/0.1 M $MnSO_4$/20wt% xanthan gum) is very sticky. When sandwiched between two glass slides, the xanthan gum electrolyte provided an adhesion that could prohibit the bottom slide from separating out when a 60-gram weight was applied, and the bottom-right photo showing the sticky xanthan gum electrolyte.

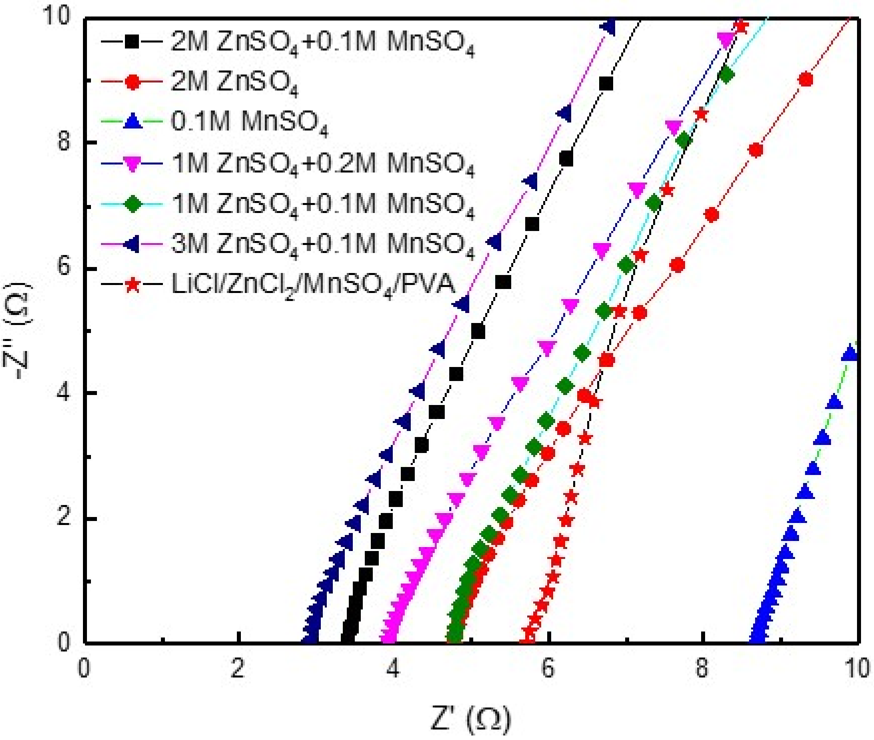

Figure S2. (a) AC impedance spectra of the xanthan gum electrolytes containing 20 wt% xanthan gum and different concentrations of sulfate salts. For comparison, the ionic conductivity of the reported $ZnCl_2$-PVA electrolyte (*Adv. Mater.* 2017, **29**, 1700274) was also measured. For impedance measurements on gum electrolytes, a piece of gum was placed between two stainless sheets of steel having an area of 4.1 cm^2, and then the gum was uniformly compressed into a 0.21-cm-thick film. Impedance measurements were carried out between 10 kHz to 0.01 Hz with an AC amplitude of 10 mV. The real impedances at the highest frequency were taken as the bulk resistance. The equation of ionic conductivity can be expressed as $\sigma = l/RA$, where σ is conductivity, and l, R, and A represent the thickness, the bulk resistance, and the area of gel polymer electrolyte, respectively. For example, the bulk resistance of the optimized xanthan gum electrolyte (20 wt% xanthan gum, 2 M $ZnSO_4$ and 0.1 M $MnSO_4$) at the highest frequency was measured as 3.41 **Ω**. Therefore, the ion conductivity was then calculated to be 1.46×10^{-2} S cm^{-1}.

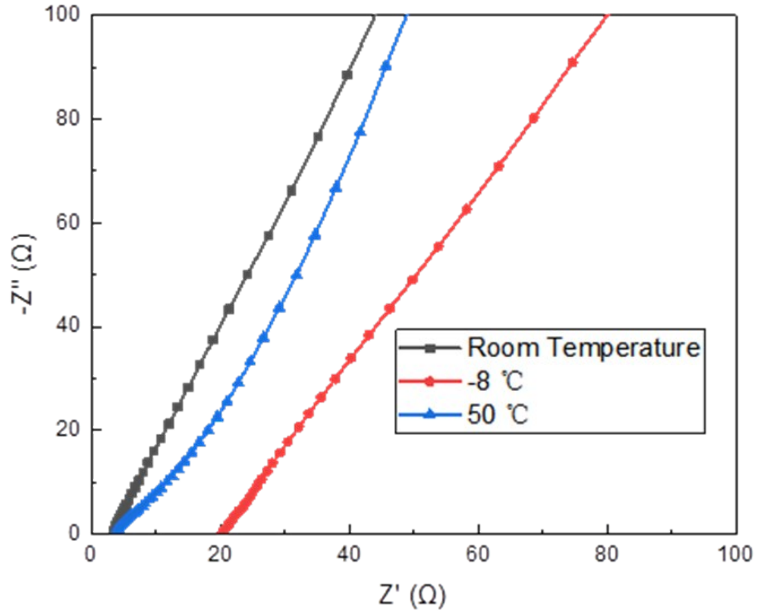

Figure S3. AC impedance spectra tested at different temperatures for the xanthan gum electrolytes containing 20 wt% xanthan gum, 2 M $ZnSO_4$ and 0.1 M $MnSO_4$.

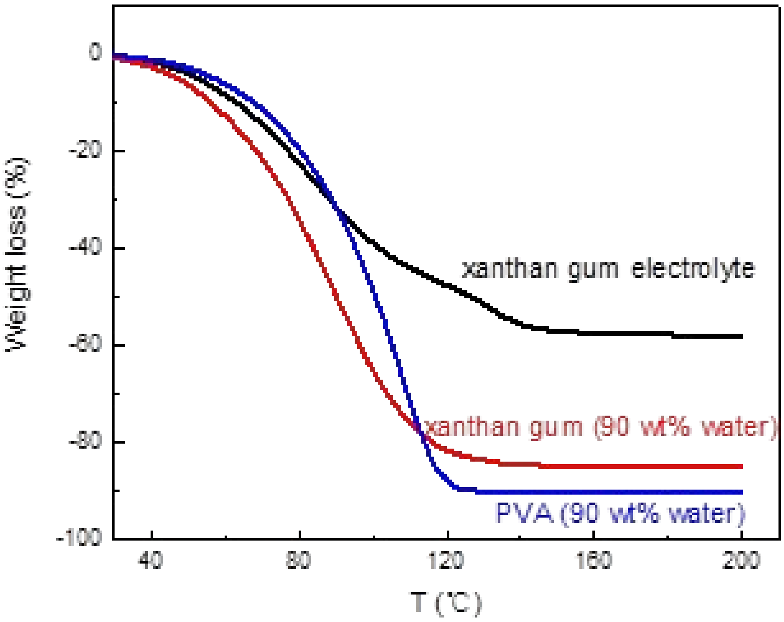

Figure S4. Thermogravimetric analysis results of 10 wt% xanthan gum, 10 wt% PVA and 20 wt% xanthan gum with 2 M $ZnSO_4$ and 0.1 M $MnSO_4$. The water contents are 90 wt%, 90 wt% and 65 wt% for these gels, respectively. When the temperature is above 120 ºC, the water in the PVA gel was totally evaporated, but the water weight percentages remained in the xanthan gum and the xanthan gum electrolyte which are about 6.5 wt% and 12 wt%, respectively, are still higher than the initial values. These comparisons indicate that xanthan gum has very strong water preservation ability.

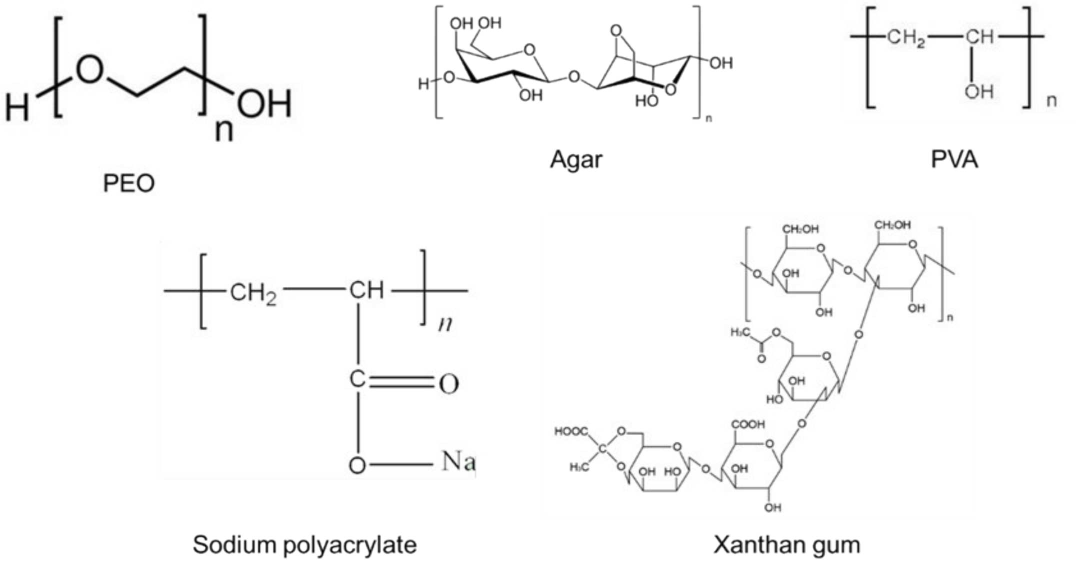

PEO

Agar

PVA

Sodium polyacrylate

Xanthan gum

Figure S5. Molecular structures of poly(ethylene oxide), agar, PVA, sodium polyacrylate and xanthan gum, respectively.

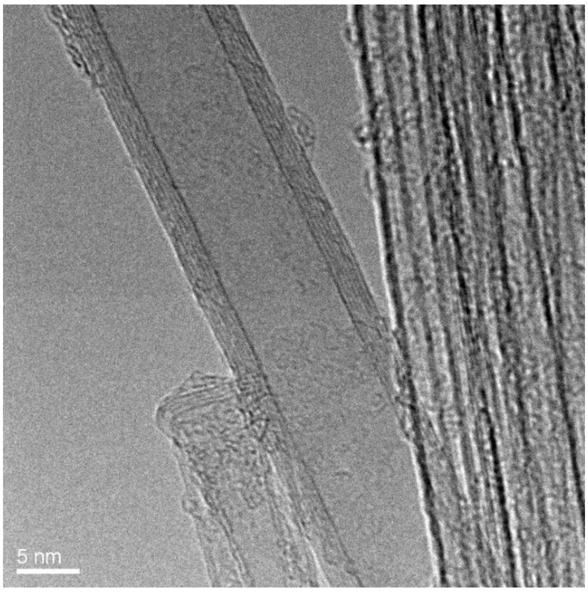

Figure S6. Typical TEM image of CNTs in presently used CNT films, which indicates that the CNTs are multiwalled and have a diameter of 10–15 nm.

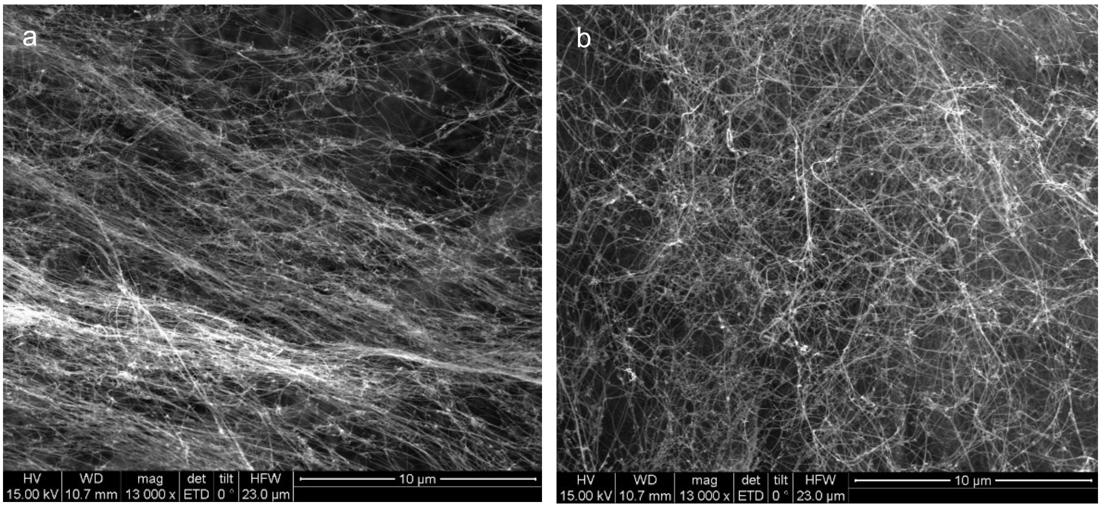

Figure S7. SEM images (a) before and (b) after electrochemical hydrophilization.

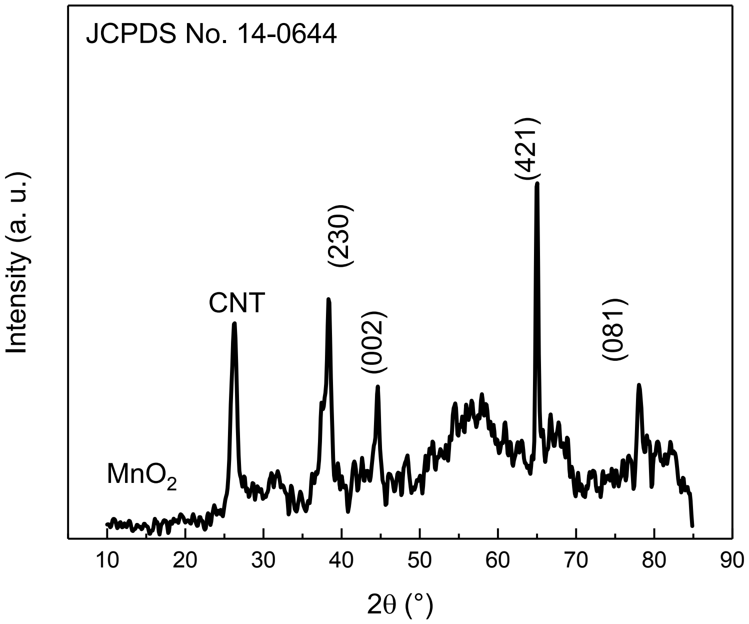

Figure S8. X-ray powder diffraction patterns of the MnO$_2$/CNT composite film. The peaks were indexed according to the PDF card (JCPDS No. 14-0644), suggesting the formation of □-MnO$_2$ on CNT films.

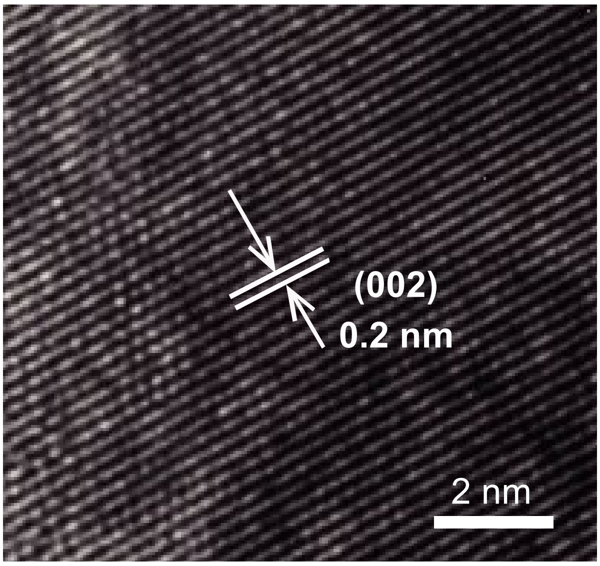

Figure S9. The high-resolution transmission electron microscopy (HRTEM) image of the MnO$_2$ electrochemically deposited on the CNT film.

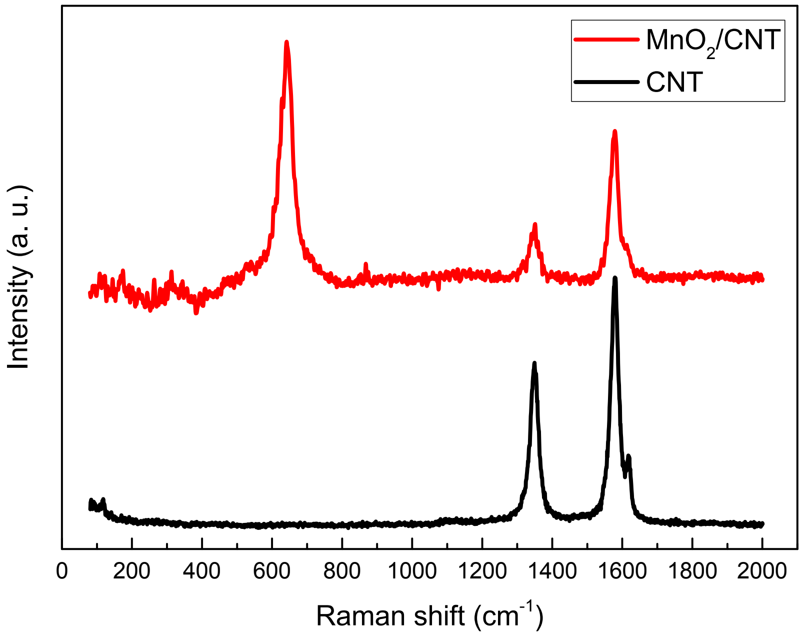

Figure S10. Raman spectra of MnO_2/CNT composite films and CNT films.

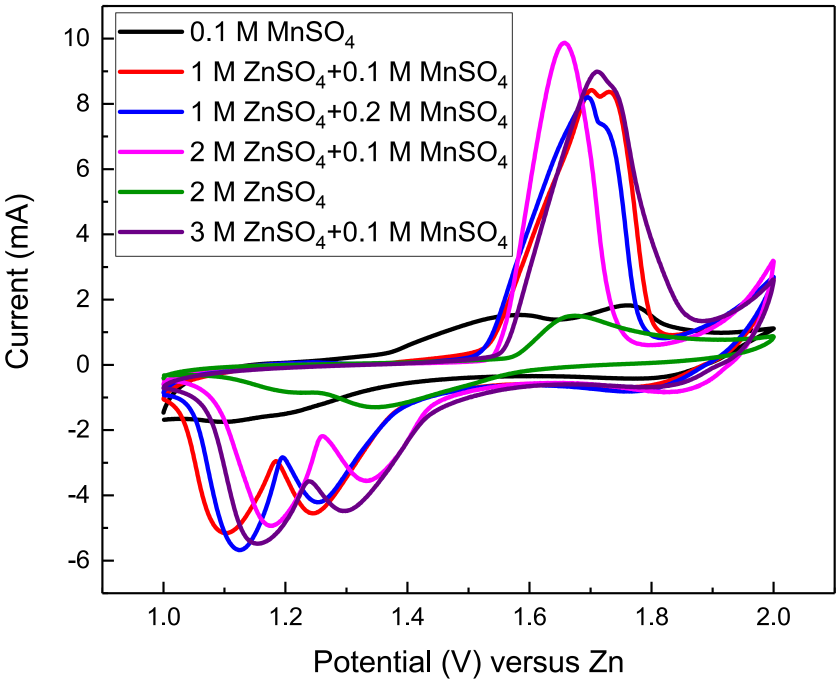

Figure S11. Cyclic voltammetry curves obtained by scanning CNT/MnO_2 composite films in aqueous electrolytes having different concentrations of $ZnSO_4$ and $MnSO_4$ between 1.0 V and 2.0 V versus a Zn foil at 1 mV s^{-1}. Among the investigated electrolytes that have different concentrations, the electrolyte containing 2 M $ZnSO_4$ and 0.1 M $MnSO_4$ enabled the highest reduction potentials, lowest oxidation potentials and thus the minimum value of ΔE_p. The capacity is low for the 0.1 M $MnSO_4$ electrolyte, which could be due to the low ion conductivity of the electrolyte and the absence of Zinc ions for insertion. The 2 M $ZnSO_4$ also enabled very low capacity possibly resulting from the formation of irreversible Mn_3O_4 (Pan et al., Nature Energy 2016, 1, 16039). Adding a proper amount of $MnSO_4$ could help stabilize the cathode by balancing Mn^{2+} dissolution and oxidation (Pan et al., Nature Energy 2016, 1, 16039). The peak potentials were associated the Zn^{2+} and H^+ insertions, and $MnSO_4$ and $ZnSO_4$ influence ion concentrations in the electrolyte.

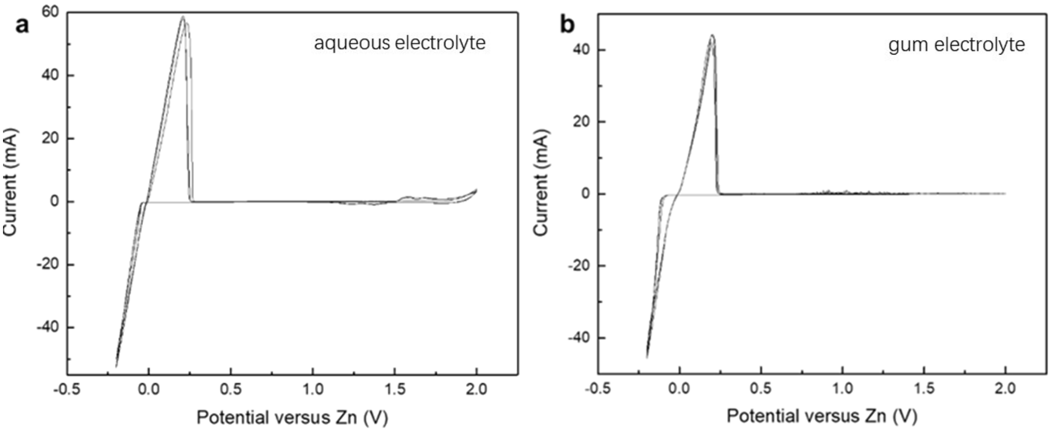

Figure S12. Cyclic voltammetry of Zn foils (2×2 cm^2) tested in the aqueous electrolyte (2 M $ZnSO_4$ and 0.1 M $MnSO_4$) and the gum electrolyte (20 wt% xanthan gum, 2 M $ZnSO_4$ and 0.1 M $MnSO_4$) at the scan rate of 0.5 mV s^{-1} between −0.2 and 2.0 V. The cyclic voltammetry performed in both the aqueous electrolyte and the gum electrolyte indicated reversible electrochemical deposition/dissolution of Zn, with coulombic efficiencies being about 100% for the gum electrolyte and about 92% for the aqueous electrolyte, respectively. The difference in coulombic efficiency could be due to the fact that Zn showed larger corrosion current in the aqueous electrolyte than that in the gum electrolyte (Figure S14). The aqueous electrolyte enabled higher current densities than the gum electrolyte and the onset potential of Zn ion deposition for the aqueous electrolyte was lower than that for the gum electrolyte. These can be explained by the high ion conductivity of the aqueous electrolyte (5.6 S/m) compared with that of the gum electrolyte (1.46 S/m). The gum electrolyte enabled a wider electrochemical window than the aqueous electrolyte, possibly due to the difference in ion conductivity and the reduced effective contact area between the gum electrolyte and the zinc foil compared with that for the aqueous electrolyte.

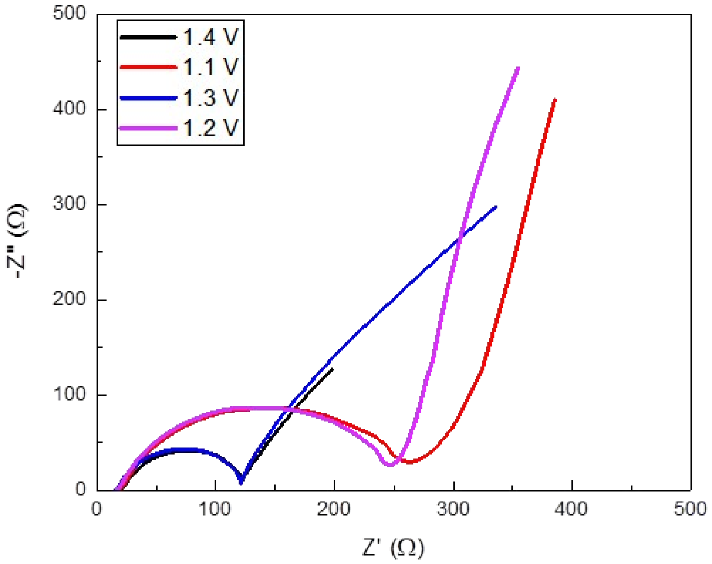

Figure S13. Electrochemical impedance spectroscopy taken at different voltages (versus Zn) for a gum Zn–MnO_2 battery. The voltage points at 1.3 V and 1.4 V are in the range of the plateau I and the voltage points at 1.1 V and 1.2 V are in the range of plateau II, respectively. The battery showed very similar results in terms of ohm resistance and charge transfer resistance in the range of the same plateau. The ohm resistances were almost identical at the two plateaus but the charge transfer resistance at the plateau I was much lower than that at the plateau II. This indicates a different ion intercalation mechanism at the two plateaus. Considering the size difference between H^+ and Zn^{2+}, the plateau I at the high voltage range and the plateau II at the low voltage range has been assigned to H^+ and Zn^{2+} insertions, respectively (W. Sun, F. Wang, S. Hou, C. Yang, X. Fan, Z. Ma, T. Gao, F. Han, R. Hu, M. Zhu, C. Wang, *J Am Chem Soc* **2017**, *139*, 9775.).

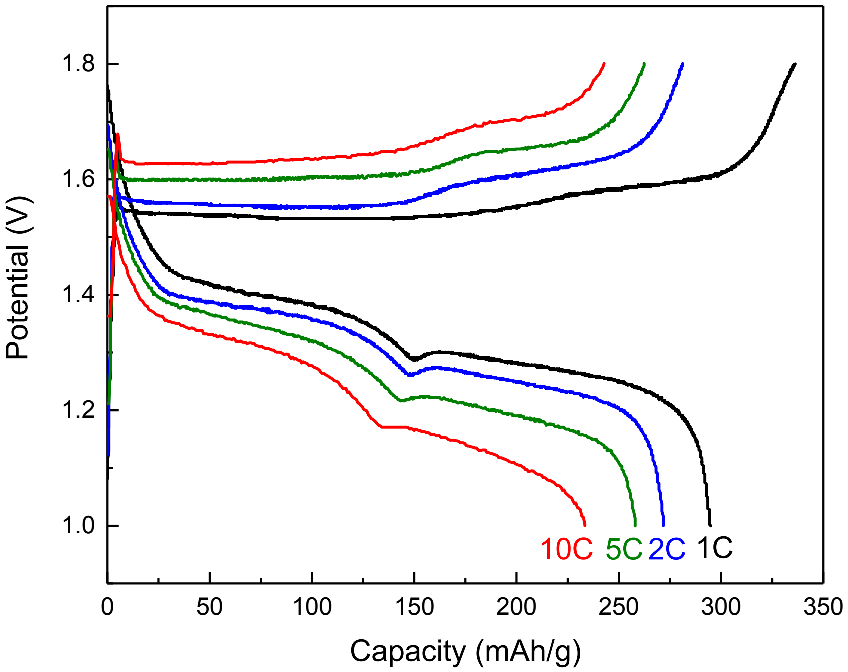

Figure S14. Galvanostatic charge/discharge profiles at different rates from 1C to 10C tested in aqueous electrolyte.

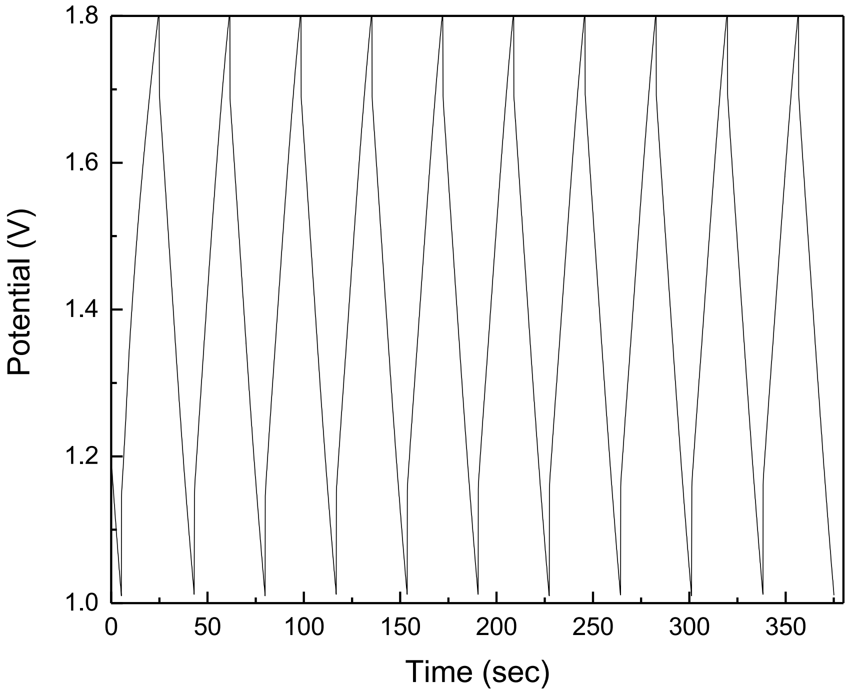

Figure S15. Galvanostatic charge-discharge curves of CNT electrodes using electrolyte 2 M $ZnSO_4$ +0.1 M $MnSO_4$ at 1 mA. The capacity contribution of CNT film is only 2.6 mAh/g.

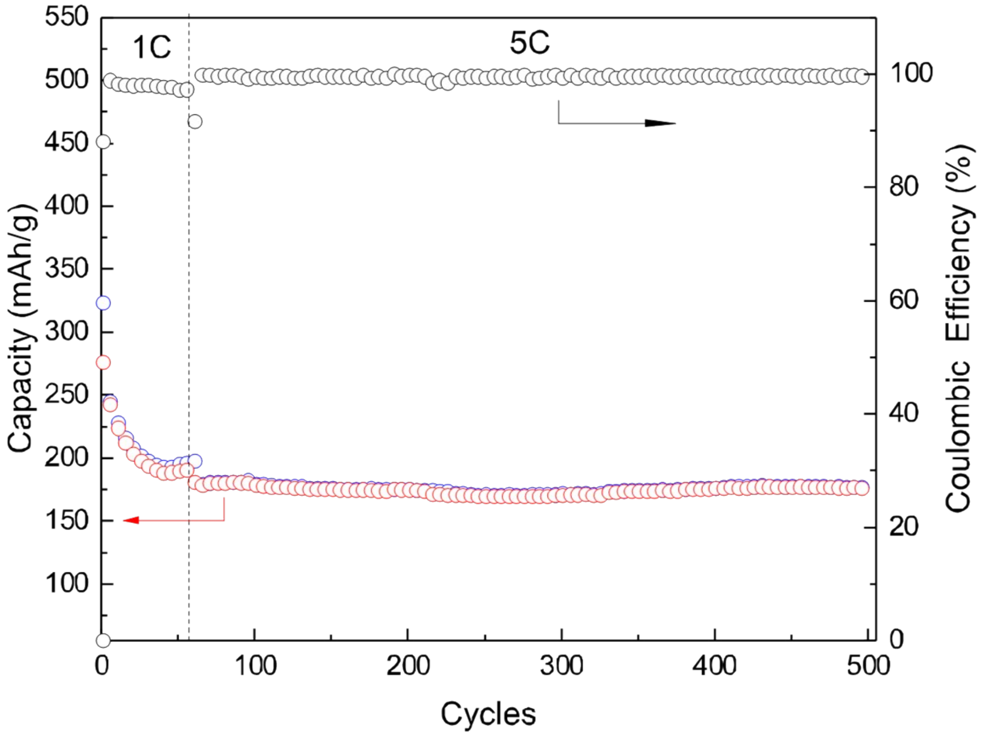

Figure S16. Galvanostatic charge/discharge profiles at 1C and 5C tested in aqueous electrolyte. The specific capacity could maintain 190 mAh g^{-1} at 1C after 60 cycles and 180 mAh g^{-1} at 5C after 440 cycles.

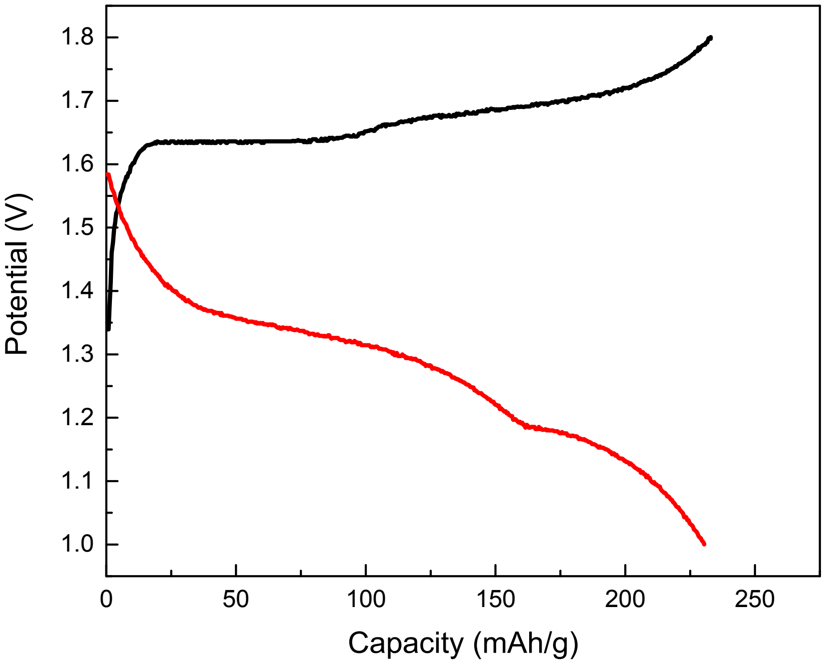

Figure S17. Galvanostatic charge/discharge curves at 5C of a Zn–MnO_2 battery with a Zn/MnO_2 mole ratio of 2. Zinc were electrochemically deposited on a current collector. And the gravimetric energy density based on the mass of cathode and anode is 88 Wh kg^{-1}.

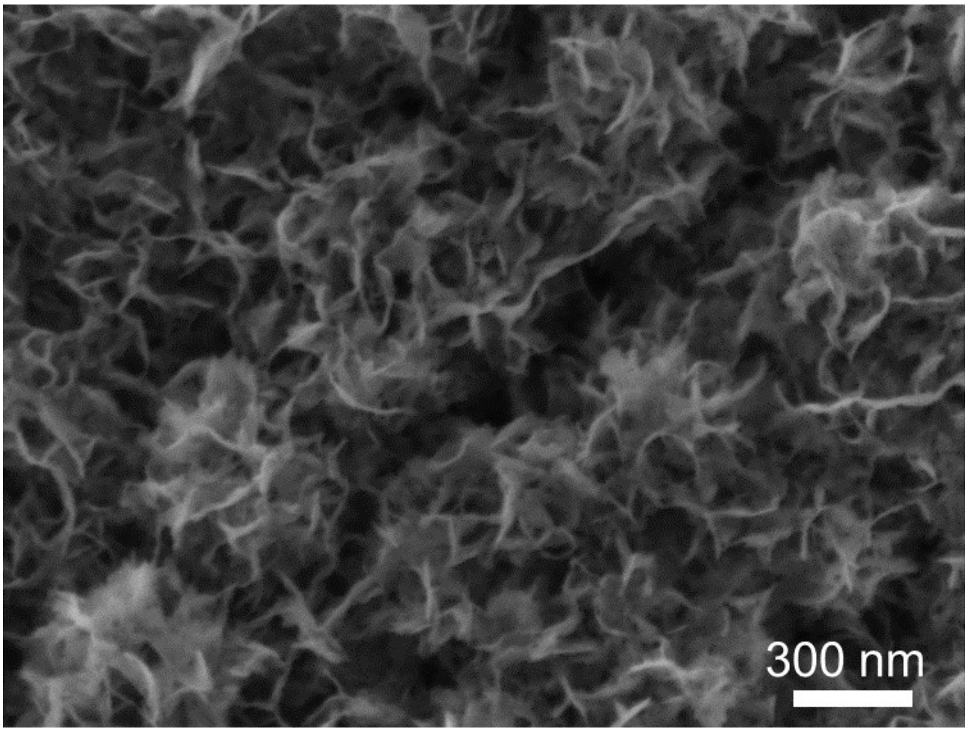

Figure S18. SEM of a MnO_2 cathode after 300 charge/discharge cycles at 1C.

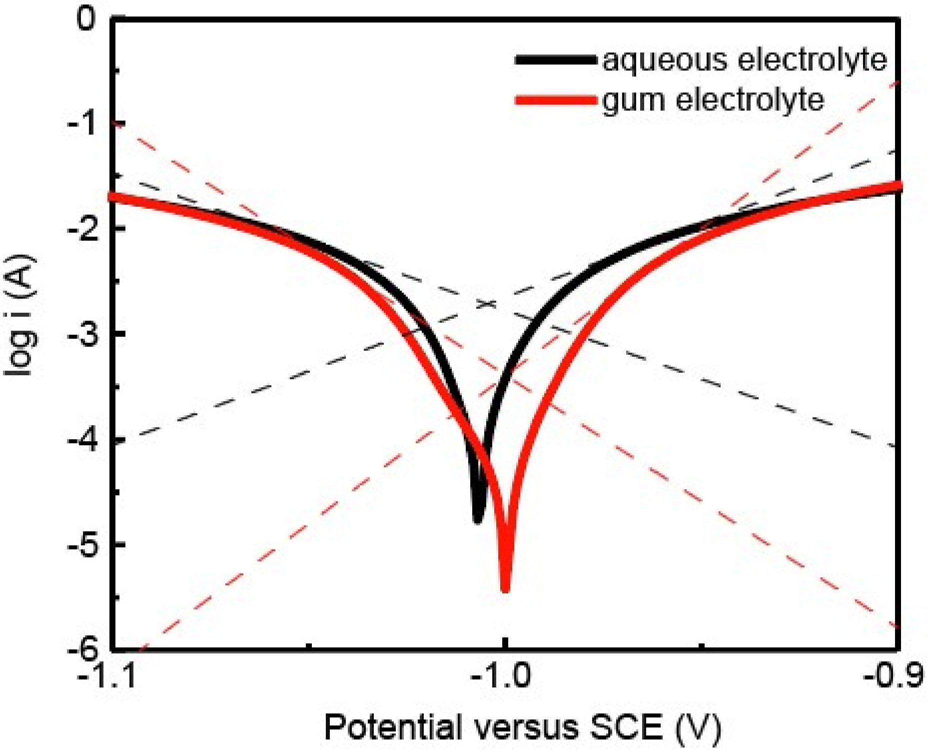

Figure S19. Tafel plots for the Zn foils tested in the aqueous electrolyte (2 M $ZnSO_4$ and 0.1 M $MnSO_4$) and the gum electrolyte (20 wt% xanthan gum, 2 M $ZnSO_4$ and 0.1 M $MnSO_4$). The corrosion potentials of zinc foils were −1.007 V and −1 V versus SCE in the aqueous electrolyte and gum electrolyte, respectively. The intercept of the two-linear segment of the Tafel slope. Extrapolating the linear portions of the logarithmic current versus potential plot gives an intersection and the current value at this intersection is the corrosion current. As shown in Figure S14, the corrosion current of the Zn foil in the aqueous electrolyte was 2.02 mA and the Zn foil in xanthan gum electrolyte was 0.4 mA, which indicates that the xanthan gum electrolyte could help slow down the self-corrosion of Zn foils in such mildly acidic electrolyte.

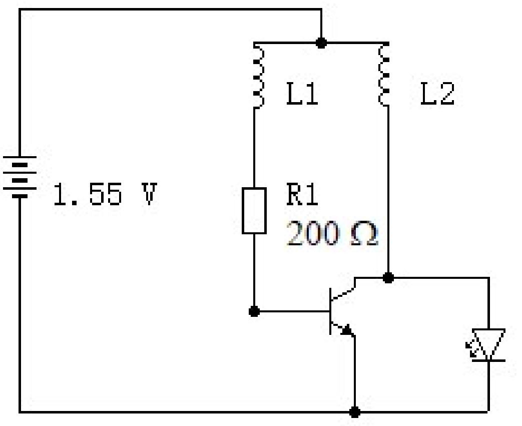

Figure S20. A joule thief circuit driving a red LED. The coil consists of a standard ferrite toroid core with two windings of 20 turns each. The battery voltage is usually 1.5 V. The resistor is ~200 kΩ. The type of transistor is S8050.

Table S1. Comparison of the ion conductivities of zinc ion polymer electrolytes

Salts	Polymer matrix	Ionic conductivity (S/m)	References	Electrolyte concentration
$ZnSO_4$	Xanthan gum	1.03	this work	2 M $ZnSO_4$
$MnSO_4$	Xanthan gum	0.5	this work	0.1 M $MnSO_4$
$ZnSO_4$/ $MnSO_4$	Xanthan gum	0.95	this work	1 M $ZnSO_4$ +0.1 M $MnSO_4$
$ZnSO_4$/ $MnSO_4$	Xanthan gum	1.23	this work	1 M $ZnSO_4$ +0.2 M $MnSO_4$
$ZnSO_4$/ $MnSO_4$	Xanthan gum	1.46	this work	2 M $ZnSO_4$ +0.1 M $MnSO_4$
$ZnSO_4$/ $MnSO_4$	Xanthan gum	1.65	this work	3 M $ZnSO_4$ +0.1 M $MnSO_4$
$ZnSO_4$/ $MnSO_4$	HPE	1.76	*Energy Environ. Sci.,* 2018	HPE was electrospun and soaked in 2 M $ZnSO_4$ +0.1 M $MnSO_4$
$ZnSO_4$/ $MnSO_4$	Gelatin	0.568	*Energy Environ. Sci.,* 2018	Gelatin was electrospun and soaked in 2 M $ZnSO_4$ +0.1 M $MnSO_4$
$ZnCl_2$	PEO	< 0.01	*Solid State Ionics,* 2005, **176,** 1797.	
$ZnCl_2$	PEO	0.2~0.4	*J. Electrochem.Soc.,* 2007, **154,** A554	prepared using PEO γ-irradiated by a selected dose of 309 kGy and TiO2 nanograins
$Zn(CF_3SO_3)_2$	Poly-ε-caprolactone	8.8×10^{-4}	*Express Polym. Lett.,* 2013, **7,** 495	25 wt.% $Zn(CF_3SO_3)_2$
$Zn(ClO_4)_2$	Poly(4-vinylpyridine)	2×10^{-6}	*Macromolecules,* 2004, **37,** 192	50 wt.% $Zn(ClO_4)_2$
$LiCl/ZnCl_2$/ $MnSO_4$	PVA	0.897	*Adv. Mater.* 2017, **29**, 1700274	3 M LiCl+2 M $ZnCl_2$+0.4 M $MnSO_4$

Table S2. The molecular weight of xanthan gum electrolyte storage before and after 1 year

	M_n (g/mol)	M_p (g/mol)	M_w (g/mol)	M_z (g/mol)
Fresh electrolyte	4.098×10^5 (±0.552%)	4.365×10^5 (± 0.498%)	4.593×10^5 (± 0.758%)	5.230×10^5 (± 2.033%)
Electrolyte stored for one year	5.000×10^5 (±0.838%)	4.933×10^5 (±0.705%)	5.582×10^5 (±1.261%)	6.326×10^5 (±3.464%)

Note: a) M_n, M_p, M_w, and M_z refer to number-average molecular weight, peak molecular weight, weight-average molecular weight, and Z-average molecular weight, respectively. The unit is g/mol. b) The number in the bracket refers to deviation.

Table S3. **Comparison of the battery properties**

Cathode	Morphology	Electrolyte	Charge/discharge potential range	Specific capacity (mAh/g)	Ref.
α-MnO_2	—	1 M $ZnSO_4$	1-1.9 V	210 (0.5C)	*Angew. Chem.*, 2012, **124**, 957
α-MnO_2	nanorod	2 M $ZnSO_4$ + 0.5 M $MnSO_4$	1-1.9 V	140 (1.6C)	*Electrochimica Acta.*, 2014, **133**, 254.
α-MnO_2	nanorod	2 M $ZnSO_4$ + 0.1 M $MnSO_4$	1-1.8 V	285 (C/3)	*Nat. Energy*, 2016, 1,16039
$ZnMn_2O_4$	nanoparticles	3 M $Zn(CF_3SO_3)_2$	0.8-1.9 V	150 (50 mA/g)	*J. Am. Chem. Soc.*, 2016, **138,** 12894.
β-MnO_2	nanorod	3 M $Zn(CF_3SO_3)_2$ + 0.1 M $Mn(CF_3SO_3)_2$	0.8-1.9 V	213(1.62C)	*Nat. Communn.*, 2017, **8**, 405.
N-doped C/MnO_2	nanorod	3 M LiCl + 2 M $ZnCl_2$ +0.1 M $MnSO_4$	1-1.8 V	328 (0.5 A/g) (solid-state)	*J. Mater. Chem. A*, 2017, **5**, 14838
MnO_2/PEDOT	Hierarchical structure	3 M LiCl + 2 M $ZnCl_2$ +0.1 M $MnSO_4$	1-1.8 V	282.4 (0.37 A/g) (solid-state)	*Adv. Mater.* 2017, **29**, 1700274
CuHCF	nanoparticle	20 mM $ZnSO_4$	0.3-1.4 V vs SHE	52.5 (1C)	*ChemSusChem*, 2015, **8,** 481
VS_2	layered structure	$ZnSO_4$	0.4-1 V	190.3 (0.05 A/g)	*Adv. Energy Mater.*, 2017, **7**, 1601920.
$H_2V_3O_8$	nanowire	3 M $Zn(CF_3SO_3)_2$	0.2-1.6 V	423.8 (0.1 A/g)	*Small*, 2017, **13**, 1702551.
$Zn_xMo_{2.5+y}VO_{9+z}$	nanorod	0.2 M $Zn(CF_3SO_3)_2$ in propylene carbonate (PC)/dimethylsulfoxide (DMSO) (1 : 4)	0-1.6 V	220 (2 mA/g)	*J. Mater. Chem. A*, 2016, **4**, 18737
$Zn_3[Fe(CN)_6]_2$	nanoparticle	1 M $ZnSO_4$	0.8—2 V	65.4 (1C)	*Adv. Energy Mater.* 2014, 1400930
$Zn_{0.25}V_2O_5 \cdot nH_2O$	nanobelt	1 M $ZnSO_4$	0.5-1.4 V	282 (300 mA/g)	*Nature Energy* 2016, **1**, 16119
γ-MnO_2	Hierarchical structure	2 M $ZnSO_4$ + 0.1 M $MnSO_4$	1-1.8 V	295(aqueous), 282(solid-state) (1C)	**This work**

Note: a: The reported capacity value exceeds the theoretical capacity of 308 mAh g^{-1} (based on the molecular weight MnO_2 and one electron transfer reaction) and this could be due to the fact that this capacity contribution (70 mAh/g) from the nitrogen-doped carbon fiber cloth current collector was added but its mass was ignored.